Automatica 75 (2017) 77–87

Contents lists available at ScienceDirect

Automatica

journal homepage: www.elsevier.com/locate/automatica

Leader following trajectory planning: A trailer-like approach ☆

Pedro O. Pereira [d], Rita Cunha [b], David Cabecinhas [a,b], Carlos Silvestre [a,b], Paulo Oliveira [c,b]

[a] Department of Electrical and Computer Engineering, Faculty of Science and Technology, University of Macau, China
[b] Institute for Systems and Robotics, Instituto Superior Técnico, Universidade de Lisboa, Lisboa, Portugal
[c] Department of Mechanical Engineering, Instituto Superior Técnico, Universidade de Lisboa, Lisboa, Portugal
[d] Royal Institute of Technology, Automatic Control, Stockholm, Sweden

ARTICLE INFO

Article history:
Received 10 September 2014
Received in revised form
25 January 2016
Accepted 30 July 2016

Keywords:
Multi-vehicle trajectory planning
Leader-following
Nonlinear systems

ABSTRACT

In this paper, a trajectory planner for n autonomous vehicles following a common leader is presented, with the planning being accomplished in real time and in a three dimensional setting. The trajectory planner is designed such that n follower vehicles behave as n distinct points of a unique two dimensional trailer attached to a single leader vehicle. We prove that for a wide range of initial conditions the trailer reference frame converges to a unique solution, meaning that convergence to a fixed formation of $n+1$ vehicles is guaranteed and each follower can plan its trajectory independently from its peers, thereby reducing the need for communication among vehicles. Bounds on the planned velocity and acceleration, provide conditions for the feasibility of the planned trajectory. An experimental validation of the planner's behavior is presented with quadrotor vehicles, demonstrating the richness of the planned trajectories.

1. Introduction

Robot coordination has been the scope of a significant amount of research over the last decade. Coordination of multiple vehicles is particularly useful in a variety of applications, such as mapping, coverage, and surveillance of large areas like the sea floor (Bellingham & Rajan, 2007; Yamaguchi, 2002), providing results in a faster and more efficient manner. Coordinated motion is also required in transportation via multiple vehicles, in cases where the payload capacity of an individual vehicle is surpassed (Fink, Michael, Kim, & Kumar, 2011). Sensing robots moving in a coordinated manner can also be perceived as a distributed network of sensors, altogether accomplishing a larger sensing task or alternatively providing robustness to sensor loss in critical environments (Summers, Yu, & Anderson, 2008).

Different approaches to formation control have been proposed in the literature. In a behavior based approach, a desired behavior results from a weighting between different goal oriented behaviors but guaranteeing convergence to a desired configuration proves to be difficult (Balch & Arkin, 1999; Lawton, Beard, & Young, 2003). In a virtual structure approach (Do & Pan, 2007), the vehicles move as points of a virtual rigid body, whose motion is prescribed in a global manner. An alternative, locally defined, method is leader following, which is the one we tackle in this paper.

In the leader–follower approach to formation control, the objective is for a follower vehicle to remain at a fixed relative position, in a given reference frame, w.r.t. the leader vehicle. The problem is completely characterized by the relative position vector and the reference frame where it is defined. The choice of reference frame plays an important role in the definition of the follower's trajectory and in the sensory information necessary for computing such trajectory.

Several leader following strategies have been proposed in the literature. The simplest approach to leader following is to specify the relative position vector in the inertial reference frame as in Wen, Peng, Yu, and Rahmani (2012). The planned trajectory is simple in the sense that both the leader and the follower describe an identical path, apart from a translation. Because the follower's path can overlap with the leader's path, a reduced efficiency gain resulting from the use of multiple vehicles is expected.

Defining the relative position vector in a reference frame attached to the leader, such as the leader's Serret–Frenet frame, results in follower trajectories with more complex behavior. This approach has been proposed by several authors (Cui, Sam Ge, How, & Choo, 2010; Mariottini, Morbidi, Prattichizzo, Pappas, &

☆ The material in this paper was partially presented at the 53rd IEEE Conference on Decision and Control, December 15–17, 2014, Los Angeles, CA, USA. This paper was recommended for publication in revised form by Associate Editor Tamas Keviczky under the direction of Editor Christos G. Cassandras.

E-mail addresses: ppereira@isr.ist.utl.pt (P.O. Pereira), rita@isr.ist.utl.pt (R. Cunha), dcabecinhas@isr.ist.utl.pt (D. Cabecinhas), cjs@isr.ist.utl.pt (C. Silvestre), pjcro@isr.ist.utl.pt (P. Oliveira).

http://dx.doi.org/10.1016/j.automatica.2016.09.001
0005-1098/

Daniilidis, 2007; Peng, Wen, Rahmani, & Yu, 2013) and because the chosen reference frame is uniquely defined, no convergence analysis is required. However, its implementation requires more information than should be expected, since vehicle control at the velocity level requires the knowledge of the leader's velocity and acceleration (in the form of the angular velocity of the Serret–Frenet reference frame).

Other alternatives to formation control in a two dimensional setting that use a leader following approach are proposed in Justh and Krishnaprasad (2004) and Leonard and Fiorelli (2001), where attractive and repulsive interactions are designed such that a certain inter-vehicle spacing is attained. However, the final vehicles' configuration is not unique in the sense that it depends on the initialization of the formation.

In this paper, we design a physically inspired leader following strategy where the follower mimics the behavior of a point on a rigid-body trailer attached to the leader. The work shares similarities with those in Consolini, Morbidi, Prattichizzo, and Tosques (2008) and Roldão, Cunha, Cabecinhas, Oliveira, and Silvestre (2013), however we provide new and rigorous proofs on the convergence to a unique formation for n followers and specify bounds that can be used in studying the feasibility of the planned trajectory.

We propose a two part solution to the leader–follower formation problem. First, a desired trajectory is computed for an ideal follower vehicle, hereafter called *virtual* follower, with the help of the proposed trajectory planner. The planned trajectory is then used as a reference to a trajectory tracking controller that drives the *real* follower vehicle to the *virtual* follower. In this paper, we focus on the problem of generating the follower trajectory and providing conditions for its feasibility. We also present experimental results for the complete planning/tracking problem using quadrotor vehicles.

Quadrotors are aerial vehicles ideal for testing algorithms, due to their simplicity, high maneuverability, hover capability, and ability to track any position trajectory within the limits of their actuation dynamics. Tracking controllers for quadrotor vehicles have been extensively studied in the literature, c.f. the survey article (Hua, Hamel, Morin, & Samson, 2013), and the *virtual* follower trajectory generated by our planner can be used as reference for any generic tracking controller applied to the follower vehicle. We emphasize that, while the proposed algorithm is validated with quadrotor vehicles, its applicability is not limited to these vehicles; moreover, we highlight that quadrotor vehicles are underactuated, which does not prevent the applicability of the proposed planning strategy.

The remainder of the paper is structured as follows. Section 2 describes the main contributions and Section 3 presents some mathematical notation used throughout the paper. Section 4 describes the leader–follower problem. Section 5 derives the trajectory planner and studies its properties. Section 6 presents and examines the obtained experimental results. A preliminary and reduced version of this work was accepted for publication in the 2014 Conference on Decision and Control (Pereira, Cunha, Cabecinhas, Silvestre, & Oliveira, 2014). With respect to the preliminary version, this paper presents significantly more details on the derivation of the main theorems and provides additional results. In particular, the proposed solution is analyzed for robustness to measurement noise and a discussion is added on how to plan the leader's motion so as to lead the formation of vehicles to track a desired motion.

2. Main contributions

The solution to the problem of leader following here proposed bears similarities with those reported in Consolini et al. (2008), Peng et al. (2013) and Roldão et al. (2013). Our main contributions lie on the analysis of the collective motion that results from applying the proposed planner, which has been mostly overlooked in previous works, specially for the case of a leader vehicle describing arbitrary paths.

Firstly, we provide an intuitive explanation for the obtained motion, specifically we highlight the fact that the obtained motion is exactly that of a trailer. This means that the leader, which is responsible for leading the motion of the formation, can be regarded as a vehicle rigidly attached to a trailer, with the followers behaving as distinct points of that trailer body.

Our main result (Theorem 3) states that for a wide range of initial conditions, all trailers attached to a leader converge to one another. This means that n followers, initially attached to n different trailers, asymptotically behave as n distinct points of a common trailer. When compared with (Consolini et al., 2008; Peng et al., 2013; Roldão et al., 2013), this a significant improvement in understanding the key features of this solution, since now we can state that, under mild assumptions, convergence to a rigid formation of $n+1$ vehicles is guaranteed. An additional important consequence is that individual followers do not need to negotiate with each other because, as they follow a common leader, they will eventually agree. Follower-to-follower communication is thus not required while communication leader-to-follower might still be necessary. (We note that given proper on-board sensors, a follower might eliminate the need to communicate with the leader as well.)

This result is valid for a leader describing arbitrary paths, as long as the leader path curvature remains below a specified upper bound. For circular paths, we can derive the analytical expression for the attracting trailer trajectory (Theorem 1), while for arbitrary paths we show that a unique attracting solution exists, despite the fact that an analytical expression is not explicitly computed (Theorem 3). Intuitively, the reason for this difference is intimately related to the fact that a circular path induces an autonomous motion while an arbitrary path induces a non-autonomous motion.

Although, for the case of arbitrary paths, the analytical expression for the attracting solution remains elusive, we are nonetheless able to say what that solution *looks like*, i.e. we provide two bounding conditions on the analytical solution (Theorem 4). Obviously, these bounds collapse to one another when the arbitrary path approaches a circular path.

We also show that the planned path does not depend on the leader's speed, but rather on the direction of motion, i.e. the direction of the leader's velocity. Obviously, the planned trajectory must depend on the leader's speed.

The constraint on the leader's curvature (mentioned above) has a very clear interpretation and it should not be understood as a disadvantage. From a distance, a leader that is moving in a small circle will actually be perceived as a vehicle at rest. In such situation, the follower should also remain at rest, which is exactly what is obtained with the proposed strategy. A small circle is associated with a large curvature, whereas the *distance* is a parameter to be specified by the designer (it can be used as a sensitivity parameter, i.e. how sensitive do we want the followers to be with respect to the leader's motion). Using once again the trailer analogy, this distance will correspond to the length of the rigid link that connects the leader to the trailer (Remark 5).

In this paper, we are primarily concerned with studying the motion the followers describe when the leader is oblivious of its followers and moves independently from them. Nonetheless, we also study the dual problem of defining the motion of the leader in order for the followers to move in a specified manner. Answering this question is interesting in the sense that we can devise a trajectory for a leader that will force the formation leader+followers to move in a specified manner, which is particularly useful in a mapping scenario (e.g. what motion should a leader take such the triangular formation – leader+2 followers – moves in an arbitrary manner).

For the most part, the paper is focused on paths rather than trajectories. However, the proposed algorithm plans a trajectory

which means a feasibility study is required (real vehicles have limits on the speed and acceleration that they can attain and their reference trajectories should be defined accordingly). Given the flight envelope of the real follower vehicles, we can impose restrictions on the leader's trajectory (i.e. leader's speed and acceleration) that guarantee that any follower is able to keep up with its leader. We finish with some experiments performed using quadrotors vehicles, which demonstrate the richness of the trajectory planner as well as the feasibility of the planned trajectories.

3. Notation

The configuration of a reference frame $\{B\}$ w.r.t. a frame $\{A\}$ is represented as an element of the Special Euclidean group of order n, $({}^A_B R, {}^A\mathbf{p}_B) \in SE(n)$, where ${}^A\mathbf{p}_B \in \mathbb{R}^n$ is the position, ${}^A_B R \in SO(n)$ is the rotation matrix, and n is either 2 or 3, depending on whether the configuration is defined in a two or three dimensional space, respectively. For points in the inertial frame $\{I\}$, the superscript frame letter is often omitted, i.e. $\mathbf{p}_B \equiv {}^I\mathbf{p}_B$. A point velocity vector is denoted by $\mathbf{v}_s$ when specified in the inertial reference frame and denoted by $\mathbf{u}_s$ when specified in the reference attached to the point (both appended with a meaningful subscript s). The vectors $\mathbf{e}_i \in \mathbb{R}^n$ with $i = \{1, \ldots, n\}$ are used to denote the unit vectors from the canonical basis for $\mathbb{R}^n$. The matrix $S(x) = x[\mathbf{e}_2 \ -\mathbf{e}_1] \in \mathbb{R}^{2\times 2}$ is skew-symmetric and it satisfies $\mathbf{b}^T S(x)\ \mathbf{b} = 0$. The map $\Pi : \{\mathbf{x} \in \mathbb{R}^3 : \mathbf{x}^T\mathbf{x} = 1\} \mapsto \mathbb{R}^{3\times 3}$, where $\Pi(\mathbf{x}) = \mathbf{I} - \mathbf{x}\mathbf{x}^T$, yields a matrix that represents the orthogonal projection operator onto the subspace perpendicular to $\mathbf{x}$. We denote by $f^{(i)}(t)$ the ith time derivative of the function $f(t)$ for $i = \{1, 2, \ldots\}$, and by $C^k(\mathbb{R}^n)$ the space of functions on $\mathbb{R}^n$ with k continuous derivatives.

4. Problem statement

In a leader following problem, a leader vehicle moves freely and it is the *goal* of one or more followers to proceed so as to *see* the leader vehicle at a constant relative position. This simple problem cannot be accomplished by most *real* vehicles as full position control is not available, i.e. a *real* follower vehicle might not be able to follow a leader at all times. This inspires the introduction of a *virtual* follower vehicle as one with full position control and consequently one which can meet the leader following *goal* at all times.

As such, the goal of the *virtual* follower, or alternatively the leader following goal, is to remain at a fixed relative position w.r.t. the leader from its own point of view, such that

$$ {}^F\mathbf{p}_{L|F} \equiv {}^F_I R\,(\mathbf{p}_L - \mathbf{p}_F) \equiv \mathbf{d}, \tag{1}$$

with $\mathbf{d} \in \mathbb{R}^3$ as a constant vector. According to (1), once the kinematics of the *virtual* follower orientation, i.e. ${}^I_F R(t)$, are established then the *virtual* follower's reference frame, i.e. $\{{}^I_F R(t), \mathbf{p}_F(t)\}$, becomes completely defined. Consequently, the design challenge lies on finding an appropriate kinematic behavior for ${}^I_F R(t)$.

The *virtual* follower's position can then be considered as the desired position for a *real* follower. As such, the problem of leader following can be addressed in two steps. The primary step is that of trajectory planning which is vehicle independent and is solved with the help of a *virtual* follower. A secondary step is that of trajectory tracking which depends on the selected vehicle and its dynamics (e.g. on the mass of that vehicle) and is solved with the help of a trajectory tracking controller. Here, we focus on the problem of trajectory planning but there are bounds on the planned velocity and acceleration that can be used to guarantee that the planned trajectory is indeed feasible.

Let $\{I\} \in SE(3)$ denote an inertial reference where the third axis is aligned with the acceleration due to gravity. Additionally, consider a second inertial reference frame $\{I\}^\star$ that coincides with $\{I\}$ apart from a constant rotation, so that its configuration w.r.t. $\{I\}$ is given by $({}^I_{I^\star}R, \mathbf{0}) \in SE(3)$. The unit vector ${}^I_{I^\star}R\,\mathbf{e}_3 \equiv \mathbf{n} \in \mathbb{R}^3$ shall be selected and considered the preferred vertical direction (for example, if a leader is scanning a vertical wall, $\mathbf{n}$ should be selected as the normal to such wall). With that in mind, the leader's motion is decomposed into a planar motion living in the plane orthogonal to $\mathbf{n}$ and a motion along the direction $\mathbf{n}$, i.e.

$$ \mathbf{p}_L^{(i)} = \Pi(\mathbf{n})\,\mathbf{p}_L^{(i)} + (\mathbf{n}^T\mathbf{p}_L^{(i)})\mathbf{n}, \tag{2}$$

where the leader's Frenet reference frame $\{L\} \in SE(2)$ is associated to $\Pi(\mathbf{n})\,\mathbf{p}_L^{(i)}$. Two separate leader following strategies will be accomplished, one along the plane orthogonal to $\mathbf{n}$ and one along the direction $\mathbf{n}$, the first being one dimensional and the second being two dimensional. As such, despite being defined in a three dimensional space, the behavior of the proposed planner is that of a two dimensional planner superimposed with a planning along an orthogonal direction, the two planning strategies being independent of one another.

Next, focus on the two dimensional leader following strategy. With an obvious abuse of notation, consider the inertial reference frame $\{I\} \in SE(2)$, the leader's Frenet reference frame $\{L\}$ defined by the pair $({}^I_L R, \mathbf{p}_L) \in SE(2)$ and the *virtual* follower reference frame $\{F\}$ defined by the pair $({}^I_F R, \mathbf{p}_F) \in SE(2)$. The kinematics of the leader are given by

$$ \begin{aligned} \dot{\mathbf{p}}_L(t) &= \mathbf{v}_L(t) \equiv {}^I_L R(t)\mathbf{u}_L(t), \\ {}^I_L\dot{R}(t) &= {}^I_L R(t) S(\omega_L(t)), \end{aligned} \tag{3}$$

where $\mathbf{v}_L \in \mathbb{R}^2$ is the linear velocity expressed in inertial coordinates, $\mathbf{u}_L = \|\mathbf{v}_L\|\,\mathbf{e}_1$ (because $\{L\}$ is a Frenet reference frame) and $\omega_L \in \mathbb{R}$ is the angular velocity (for simplicity, from hereafter the leader vehicle speed will be denoted by $\mathrm{v}_L \equiv \|\mathbf{v}_L\|$). Using the path curvature $\kappa_L(t)$, the leader's angular velocity can be written as

$$ \omega_L(t) \equiv \mathrm{v}_L(t)\kappa_L(t). \tag{4}$$

The kinematics of the follower reference frame are similarly defined.

The trajectory planning here proposed is to be implemented for n followers with one common leader. The objective is for the $n+1$ vehicles to move in a cohesive manner, i.e. to move in a fixed configuration w.r.t. to some known reference frame. However, in order to minimize communications among vehicles, we require each follower to move independently of its peers, i.e. to follow the leader regardless of whether other vehicles do the same. Under certain conditions, we guarantee the $n+1$ vehicles asymptotically move in a fixed formation, with geometry determined by the distance vector $\mathbf{d}$ selected for each vehicle and the leader's path curvature κ_L, requiring at the kinematic level solely information about the leader's position and velocity expressed in their reference frame. In summary, the trajectory planning problem can be stated as follows.

Problem 1. Given a leader vehicle with kinematics described by (3) and n *virtual* follower vehicles, define the kinematics of each follower independently and based solely on the leader's position and velocity expressed in the *virtual* followers' reference frame, such that the leader following goal (1) is satisfied at all times and for all followers and such that the $n+1$ vehicles asymptotically move in a fixed formation.

Remark 1. Without loss of generality, the leader following goal can be defined as ${}^F\mathbf{p}_{L|F} \equiv {}^F_I R_{|\mathrm{d_x}}(\mathbf{p}_L - \mathbf{p}_F) \equiv \mathrm{d_x}\mathbf{e}_1$, for $\mathrm{d_x} \in \mathbb{R}^+$ and where ${}^F\mathbf{p}_{L|F}$ is the relative position between leader and

virtual follower from the *virtual* follower's point of view. In fact, if $\mathbf{d} = \mathrm{d_x} R \mathbf{e}_1$, then ${}^{I}_{F}R\,{}^{I}_{|\mathbf{d}} = R\,{}^{I}_{F}R\,{}^{I}_{|\mathrm{d_x}}$, implying that a *virtual* follower with $\mathbf{d}$ is the same as with $\mathrm{d_x}\mathbf{e}_1$ apart from a constant rotation. This rotation has no impact on the planned trajectory. Intuitively, a follower seeing a leader ahead and moving straight is the same as one seeing a leader at a right angle but moving, instead, sideways (the only difference is a 90° rotation between followers).

5. Trajectory planner

Two leader following strategies will be pursued, one along $\mathbf{n}$ and another along the plane orthogonal to $\mathbf{n}$. As such two *virtual* followers will be designed, one in a one dimensional setting, $\mathrm{p}_F^{1D} \in \mathbb{R}$, and another in a two dimensional setting $\mathbf{p}_F^{2D} \in \mathbb{R}^2$. The desired position for the *real* Follower is the combined position of both previous *virtual* Followers, i.e. $\mathbf{p}_F = {}^{I}_{I^\star}R\,[(\mathbf{p}_F^{2D})^T\ \mathrm{p}_F^{1D}]^T$, with the leader's motion also being decomposed in a one and two dimensional motions,

$$\mathbf{p}_L = {}^{I}_{I^\star}R\,[(\mathbf{p}_L^{2D})^T\ \mathrm{p}_L^{1D}]^T. \tag{5}$$

For simplicity, we drop the superscripts $1D$ and $2D$ whenever their omission introduces no ambiguity and has no impact on the comprehension of the conveyed ideas.

5.1. Motion along $\mathbf{n}$

For the one dimensional *virtual* follower, consider the leader defined by $\mathrm{p}_L^{1D} = \mathbf{n}^T\mathbf{p}_L$ (the superscript $1D$ will hereafter be dropped). The *virtual* follower is constrained to be at a constant distance $\mathrm{d_z} \in \mathbb{R}$ from the leader along the direction $\mathbf{n}$, i.e.

$$\mathrm{p}_F = \mathrm{p}_L - \mathrm{d_z}. \tag{6}$$

This planning is a static one (given $\mathrm{p}_L^{(i)}$ for $i = \{0, 1, 2, \ldots\}$ as inputs) thus n followers can independently apply the algorithm (6) and a cohesive inter-vehicle motion is guaranteed.

5.2. Motion along the plane orthogonal to $\mathbf{n}$

For the two dimensional *virtual* follower, consider the leader defined by $\mathbf{p}_L^{2D}$. Combining (2) and (5) it follows that $[(\mathbf{p}_L^{2D})^T\ 0]^T = \Pi\,(\mathbf{e}_3)\ {}^{I^\star}_{I}R\,\mathbf{p}_L$. The superscript ^{2D} will hereafter be dropped. As explained in Section 4, the design problem lies in finding kinematics that produce a natural leader following behavior. Consider a leader at rest and $\omega_F = 2\pi\ \mathrm{s}^{-1}$: for this situation, the *virtual* follower will complete a revolution around the leader every second, which is a rather unintuitive motion (in fact, one would expect that a leader at rest would result in a follower at rest).

The proposed strategy is simple and physically inspired. We model each *virtual* follower as a point of a trailer attached to the leader vehicle, as illustrated in Fig. 1. In this case, the *virtual* follower reference frame is identical to the trailer reference frame, denoted by $\{T\}$, apart from a constant position offset $\mathbf{q}$. Equivalently,

$$\mathbf{p}_F = \mathbf{p}_T + {}^{I}_{T}R\,\mathbf{q} \equiv \mathbf{p}_T + {}^{I}_{F}R\,\mathbf{q}, \tag{7}$$

where $\mathbf{p}_T$ is the trailer hinge rigidly connected to the leader, $\mathbf{q}$ represents a point in the trailer rigid body,specified in the trailer reference frame, and by definition ${}^{I}_{T}R \equiv {}^{I}_{F}R$ —see Fig. 1. (In (7), the notation ${}^{I^\star}_{T}R$ should be used instead of ${}^{I}_{T}R$ because the trailer is defined in the x-y plane of $\{I\}^\star$. With an obvious abuse of notation, but without hindering comprehension, the notation ${}^{I}_{T}R$ is used throughout this section.)

Notice that if n followers, each one with a different $\mathbf{q}$, follow a common leader, then they behave as n distinct points of a trailer rigid body as long as they share the same trailer reference frame $\{T\}$. Later, we will show that, under certain conditions,

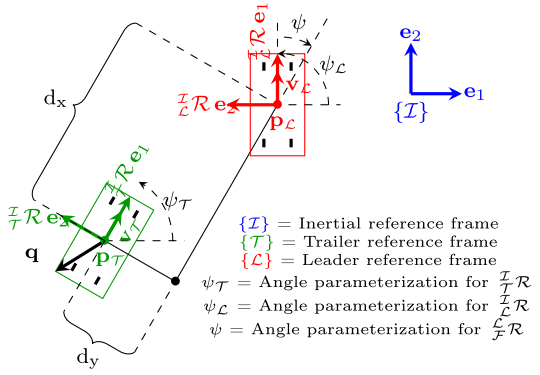

Fig. 1. Standard 1-trailer system.

there is a unique trailer reference frame to which all follower reference frames converge to. As a consequence, n followers can independently plan their trajectories and they will asymptotically behave as n points of a common trailer rigid body.

Remark 2. In a 3D setting, to avoid collisions between any two followers, the condition $[\mathbf{q}^T\ \mathrm{d_z}]_{|1} \neq [\mathbf{q}^T\ \mathrm{d_z}]_{|2}$ must be met, which is less restrictive than $\mathbf{q}_{|1} \neq \mathbf{q}_{|2}$. However, for the particular case of quadrotor vehicles, one follower should not stand in the rotor wake of another in which case (and with $\mathbf{n} = \pm\mathbf{e}_3$, i.e. $\mathbf{n}$ aligned with gravity) the latter condition becomes more significant.

A trailer vehicle is one that can only move along the axis that rigidly connects its hinge to the leader. Without loss of generality, the axis of motion is assumed to be the trailer's first axis (see Fig. 1), as such $\mathbf{v}_T \equiv {}^{I}_{T}R\,\mathbf{u}_T \equiv \mathrm{v}_T\,{}^{I}_{T}R\,\mathbf{e}_1$, where $\mathrm{v}_T \equiv \|\mathbf{v}_T\|$ is the trailer's speed. Notice that with this definition, the trailer's reference frame $\{T\}$, like the leader's $\{L\}$, becomes a Frenet reference frame. On the other hand, notice that the trailer hinge position satisfies the leader following goal (1), with

$$\mathbf{p}_L = \mathbf{p}_T + {}^{I}_{T}R\,\mathbf{d}, \tag{8}$$

and where $\mathbf{d}^T = [\mathrm{d_x}\ \mathrm{d_y}]$. Taking the time derivative of (8) yields $\mathbf{v}_L = {}^{I}_{T}R\,\mathbf{u}_T + {}^{I}_{T}RS\,(\omega_T)\,\mathbf{d}$, or equivalently,

$${}^{I}_{T}R\begin{bmatrix}1 & -\dfrac{\mathrm{d_y}}{\mathrm{d_x}}\\ 0 & 1\end{bmatrix}\begin{bmatrix}\mathrm{v}_T\\ \omega_T\,\mathrm{d_x}\end{bmatrix} = \mathbf{v}_L. \tag{9}$$

The trailer's speed is then $\mathrm{v}_T = \mathbf{e}_1{}^T\,{}^{T}_{I}R\,\mathbf{v}_L + \mathrm{d_y}\omega_T$, while the trailer's angular velocity is

$$\omega_T = \frac{\mathbf{e}_2{}^T\,{}^{T}_{I}R\,\mathbf{v}_L}{\mathrm{d_x}}. \tag{10}$$

As explained in Section 4, the kinematics of ${}^{I}_{F}R$ (which are those of ${}^{I}_{T}R$) defines the leader following behavior, thus (10) completes our planning strategy. Given that the angular velocity ω_T (and thus the kinematics of ${}^{I}_{F}R$) depend on $\mathrm{d_x}$ but not $\mathrm{d_y}$, we can assume, without loss of generality, that $\mathbf{d} = \mathrm{d_x}\mathbf{e}_1$ while the component $\mathrm{d_y}$ is incorporated in the offset $\mathbf{q}$ for each follower. For that reason, we will hereafter assume that $\mathrm{d_y} = 0$.

In what follows, we focus on analyzing the planner's behavior, more specifically we show under what conditions there is a unique attracting trailer reference frame.

Remark 3. In general, a trailer vehicle, with reference frame $\{\mathbf{p}_T,\ {}^{I}_{T'}R\}$, is one which can move along a fixed direction $\boldsymbol{\eta}$ defined in its own reference frame, i.e. $\dot{\mathbf{p}}_T = \mathrm{v}_T\,{}^{I}_{T'}R\,\boldsymbol{\eta}$. It follows that ${}^{T'}_{I}R\,[\boldsymbol{\eta}\ S\,(1)\,\boldsymbol{\eta}] \equiv {}^{T}_{I}R$, meaning that the only difference between

${}^{I}_{T'}R$ and ${}^{I}_{T}R$ (in (9)) is a constant rotation $[\boldsymbol{\eta}\ S\ (1)\ \boldsymbol{\eta}]$. This could be predicted from Remark 1, which applies to all *virtual* followers and not exclusively trailers. For the particular case $\boldsymbol{\eta} = \mathbf{e}_1$, the trailer reference frame is a Frenet reference frame.

5.3. Trajectory planner properties for 2D setting

The planning along the direction $\mathbf{n}$ is a static one, whereas the planning in the 2D space orthogonal to $\mathbf{n}$ is a dynamic one. Notice the trailer configuration with respect to $\{I\}$ belongs to the domain

$$\{({}^{I}_{T}R, \mathbf{p}_T) \in SO(2) \times \mathbb{R}^2 : \mathbf{p}_T = \mathbf{p}_L - \mathrm{d_x}\,{}^{I}_{T}R\,\mathbf{e}_1\}. \tag{11}$$

The problem at hand is simple: can we guarantee that, for a wide range of initial conditions, the trailer reference frame (11) converges to a unique (possibly time varying) reference frame. This problem shares similarities with contraction analysis, whose objective is to determine a contraction region wherein all solutions of a differential equation converge to a unique solution (Lohmiller & Slotine, 1998). We will provide conditions under which such attracting solution $\{T\}$ exists and estimate its region of attraction. As a result, if those conditions are met, we guarantee n followers can independently perform their trajectory planning while asymptotically behaving as n points of a common rigid trailer. In that case, the leader and n followers form a fixed configuration that rotates in space with the trailer reference frame.

The leader reference frame is unique, despite the trailer reference frame not being (see (11)), which is the reason for conducting all analysis w.r.t. $\{L\}$. Let ${}^{L}_{T}R$ be the rotation matrix from $\{T\}$ to $\{L\}$, parametrized by the angle $\psi = \psi_T - \psi_L$, presented in Fig. 1. In that case, the leader position w.r.t. the trailer position specified in $\{L\}$ can be rewritten as

$${}^{L}\mathbf{p}_{L|T} = \mathrm{d_x}\,{}^{L}_{T}R\,\mathbf{e}_1 = \mathrm{d_x}[\cos(\psi)\ \sin(\psi)]. \tag{12}$$

and, using (4) and (10), the kinematics of ψ can be written as

$$\dot{\psi}(t) = \omega_T(t) - \omega_L(t) = -\frac{\mathrm{v}_L(t)}{\mathrm{d_x}}(\sin(\psi(t)) + \kappa_L(t)\mathrm{d_x}). \tag{13}$$

We will show the non-autonomous system (13) (with exogenous terms $\mathrm{v}_L(t)$ and $\kappa_L(t)$) converges to a unique attracting solution for a wide range of initial conditions. This answers the problem posed in the beginning of this subsection.

Remark 4. The leader Frenet reference frame may suffer a discontinuity whenever the direction of motion, i.e. $\frac{\mathbf{v}_L}{\|\mathbf{v}_L\|}$, is discontinuous or when it is ill defined. This discontinuity is propagated to ψ and ${}^{L}\mathbf{p}_{L|T}$. For $\mathbf{v}_L(t) \in C(\mathbb{R}^2)$ with $\mathrm{v}_L \geq \mathrm{v}_L^{\min} > 0$, such discontinuities do not exist. The condition $\mathrm{v}_L^{\min} > 0$ may seem very restrictive, however notice that when the leader is at rest so is the follower, thus the vehicles cannot converge to any specific configuration. This problem can be circumvented, if instead of working in the time domain one works in the leader path parametrization domain, with respect to which the leader moves at unit speed. For simplicity, we assume the condition $\mathrm{v}_L \geq \mathrm{v}_L^{\min} > 0$ is always met.

5.3.1. Pulled vs. pushed trailer

Before we study the existence of a unique attracting solution $\psi(t)$, we present a result which is of importance in later proofs and also of interesting physical interpretation.

Lemma 1. *Consider a leader with bounded curvature satisfying* $|\kappa_L(t)\mathrm{d_x}|_\infty \leq 1 - \epsilon^2$, $\epsilon \in (0, 1]$, *and a trailer attached to such leader with kinematics described by* (13). *Then,* (i) *if* $\epsilon \neq 1$, *the set* $\Omega = \{\psi : \cos(\psi) \geq \epsilon\}$ *is positively invariant with respect to* (13) *and, for all initial conditions such that* $|\cos(\psi(0))| < \epsilon$, *the solutions of the system will enter* Ω *in finite time;* (ii) *if* $\epsilon = 1$ *and* $|\cos(\psi(0))| < 1$, $\cos(\psi)$ *converges exponentially fast to* 1.

Proof. Consider the positive definite Lyapunov function $V = 1 - \cos(\psi)$, which decreases with $\cos(\psi)$ and whose time derivative, with the help of (13), yields

$$\dot{V} = -\mathrm{v}_L\mathrm{d_x}^{-1}(\sin^2(\psi) + \sin(\psi)\kappa_L(t)\mathrm{d_x}). \tag{14}$$

If $\epsilon = 1$, $\kappa_L(t)\mathrm{d_x} = 0$ for all time and

$$\dot{V} = -\frac{\mathrm{v}_L}{\mathrm{d_x}}\sin^2(\psi) = -\frac{\mathrm{v}_L}{\mathrm{d_x}}(1 - \cos^2(\psi)) = -\frac{\mathrm{v}_L}{\mathrm{d_x}}(2 - V)V.$$

Because V decreases with $\cos(\psi)$ and $|\cos(0)| \neq 1$, it follows that $\cos(\psi)$ converges exponentially fast to 1 (however, the rate of convergence is not uniform with respect to the initial condition $\cos(0)$). Now consider $\epsilon \neq 1$ and $-\epsilon < \cos(\psi(t)) < \epsilon$ for $t \in [0\ \ T]$, which implies $\sin^2(\psi(t)) > 1 - \epsilon^2$ and $1 - \epsilon < V(t) < 1 + \epsilon \Rightarrow -(1+\epsilon) < -V(t)$ for that same time interval. Given the condition $|\kappa_L(t)\mathrm{d_x}|_\infty \leq 1 - \epsilon^2$ it then follows that (14) satisfies

$$\begin{aligned}\dot{V} &\leq -\mathrm{v}_L\mathrm{d_x}^{-1}\left(\sin^2(\psi) - |\sin(\psi)\kappa_L(t)\mathrm{d_x}|\right)\\ &\leq -\frac{\mathrm{v}_L}{\mathrm{d_x}}(1-\delta)(1+\cos(\psi))V\\ &\quad -\frac{\mathrm{v}_L}{\mathrm{d_x}}\delta\,|\sin(\psi)|\left(|\sin(\psi)| - \frac{1-\epsilon^2}{\delta}\right)\end{aligned}$$

which means that if we take $\delta = \sqrt{1-\epsilon^2}$ and remembering that $\sin^2(\psi(t)) > 1 - \epsilon^2$, then

$$\begin{aligned}\dot{V} &< -\mathrm{v}_L\mathrm{d_x}^{-1}(1-\delta)(1+\cos(\psi))V\\ &< -\mathrm{v}_L\mathrm{d_x}^{-1}(1-\sqrt{1-\epsilon^2})(1-\epsilon)V \quad \forall t \in [0\ \ T],\end{aligned}$$

and consequently, V (which is contained in $(1-\epsilon\ \ 1+\epsilon)$) must decrease until $V \leq 1 - \epsilon$. Equivalently, there exists a finite time T such that $\cos(\psi(t)) \geq \epsilon$ for all $t > T$ (remember that $V(t)$ decreases with $\cos(\psi(t))$). □

Corollary 1. *Consider a leader with bounded curvature satisfying* $|\kappa_L(t)\mathrm{d_x}|_\infty < 1$, *and a trailer attached to such leader with kinematics described by* (13). *Then, the set* $\{\psi : \cos(\psi) > 0\}$ *is positively invariant w.r.t.* (13).

Notice, from (12), that $\mathbf{e}_1{}^{T}{}^{L}\mathbf{p}_{L|T} = \mathrm{d_x}\cos(\psi)$. Then, Lemma 1 has a very interesting physical interpretation. It says that given an upper bound on the curvature (whose interpretation will be provided later) and a proper initialization, the trailer will be forever pulled after a finite time, i.e. $\mathbf{e}_1{}^{T}{}^{L}\mathbf{p}_{L|T}(t) > 0$ for $t > T$. In a weaker form, Corollary 1 says that if a trailer is initially being pulled then it will be forever pulled. Lemma 1 does not consider the case $\kappa_L\mathrm{d_x} = 1$ ($\epsilon = 0$), which shall be studied later on.

5.3.2. Leader path with constant curvature

We now consider the simplest case where a leader describes a circular or rectilinear path. For these paths, the curvature is constant and we prove that ψ has a unique almost global exponentially stable equilibrium point $\psi^\star$ for $\kappa_L\mathrm{d_x} < 1$, a unique equilibrium point $\psi^\star$ for $\kappa_L\mathrm{d_x} = 1$ (not asymptotically stable) and no equilibrium points for $\kappa_L\mathrm{d_x} > 1$.

A quick analysis of Eq. (13) reveals that if κ_L is a constant satisfying $\kappa_L\mathrm{d_x} < 1$then two equilibrium points exist,

$$\cos(\psi^\star) = +\sqrt{1 - (\kappa_L\mathrm{d_x})^2} \wedge \sin(\psi^\star) = -\kappa_L\mathrm{d_x}, \tag{15a}$$

$$\cos(\psi^\dagger) = -\sqrt{1 - (\kappa_L\mathrm{d_x})^2} \wedge \sin(\psi^\dagger) = -\kappa_L\mathrm{d_x}. \tag{15b}$$

Lemma 1 suggests that an equilibrium point can only be stable if it satisfies $\cos(\psi) > 0$. Notice that for a leader describing a rectilinear path (one dimensional motion), i.e. $\kappa_L = 0$, the equilibrium solutions are $\{{}^{L}\mathbf{p}^{\star}_{L|T}, {}^{L}\mathbf{p}^{\dagger}_{L|T}\} = \{\cos(\psi^\star)\mathrm{d_x}, \cos(\psi^\dagger)\mathrm{d_x}\} = \pm\mathrm{d_x}$; these are exactly the equilibrium solutions one would obtain for a one

dimensional leader following strategy, but while in a one dimensional setting both solutions are stable, in a two dimensional trailer setting only one solution is stable. If $\kappa_L \mathrm{d_x} = 1$ then *only one* equilibrium solution exists ($\cos(\psi^\star) = 0 \wedge \sin(\psi^\star) = -1$) and its stability shall be studied separately. The system (13) also reveals that no equilibrium solution exists for $\kappa_L \mathrm{d_x} > 1$, with a very clear interpretation. According to (10), ω_T is bounded by $\frac{\mathrm{v}_L}{\mathrm{d_x}}$ whereas $\omega_L = \mathrm{v}_L \kappa_L$; this means that if $\mathrm{d_x}$ is too large (compared with the leader path radius or κ_L^{-1}) the trailer will not have enough angular velocity to keep up with the leader's rotation. In that case, ${}^L_T R$ can never reach an equilibrium solution.

Remark 5. The absence of an equilibrium solution for $\kappa_L \mathrm{d_x} > 1$ should not be interpreted as a disadvantage but rather as an advantage. A leader describing a path with $\kappa_L \mathrm{d_x} \gg 1$ is a leader which is almost at rest w.r.t. the trailer and we do not want the *virtual* follower to rotate with the leader but rather to stay at rest (in which case ψ has no equilibrium solution). The parameter $\mathrm{d_x}$ is thus the tuning parameter we have described in the Section 2: a bigger $\mathrm{d_x}$ means the followers will be less sensitive to leader motions (increasing the distance to the leader has the effect of reducing, from the trailer's perspective, the "size" of the path described by the leader).

Theorem 1. *Consider a leader describing a path with constant curvature satisfying $\kappa_L \mathrm{d_x} < 1$ and a trailer attached to such leader with kinematics described by (13). Let $\psi^\star$ and $\psi^\dagger$ be given by (15a) and (15b), respectively. If $\psi(0) \neq \psi^\dagger$ then $\psi(t)$ converges exponentially fast to the stable equilibrium point $\psi^\star$, i.e. (13) has an almost globally exponentially stable (AGES) equilibrium point at $\psi = \psi^\star$.*

Proof. Consider the positive semi-definite Lyapunov function $V(t) = \frac{1}{2}(\sin(\psi(t)) + \kappa_L \mathrm{d_x})^2$, which is positive everywhere expect for the two equilibrium points $\psi^\star$ and $\psi^\dagger$ and bounded, more specifically $V(t) < 2$ for all t. From (13) and recalling that $\dot{\kappa}_L = 0$, the Lyapunov time derivative yields

$$\dot{V}(t) = -2\mathrm{v}_L(t)\mathrm{d_x}^{-1}\cos(\psi(t))V(t), \tag{16}$$

and consequently

$$V(T) = V(0)\exp\left(\int_0^T -2\mathrm{v}_L(\tau)\mathrm{d_x}^{-1}\cos(\psi(\tau))d\tau\right), \tag{17}$$

where $V(0) \neq 0$ from the conditions of the Theorem. We can divide the state domain in three sets, $\Omega_1 = \{\psi : \cos(\psi) \geq \epsilon\}$, $\Omega_2 = \{\psi : |\cos(\psi)| < \epsilon\}$ and $\Omega_3 = \{\psi : \cos(\psi) \leq -\epsilon\}$, noting that the union of these sets forms the whole domain and $\psi^\star$ belongs to the interior of Ω_1, whereas $\psi^\dagger$ is in the interior of Ω_3. According to Lemma 1, Ω_1 is positively invariant meaning that if $\psi(0) \in \Omega_1$ then $\dot{V}(t) < -\alpha V(t)$ for $t > 0$ and $\alpha > 0$ and $V(t)$ converges exponentially fast to the origin and to the equilibrium point in (15a). Also, according to Lemma 1, if $\psi(0) \in \Omega_2$ then $\psi(t)$ will enter Ω_1 in finite time, meaning that convergence is also guaranteed. Finally, if $\psi(0) \in \Omega_3$ and $\psi(0) \neq \psi^\dagger$ it follows from (17) that $V(t) > V(0)\exp\left(2\frac{\mathrm{v}_L^{\min}}{\mathrm{d_x}}\epsilon t\right)$, meaning that exists a time T such that $V(T) \geq 2$. As this is not possible, the logical consequence is that the $\psi(t)$ must enter Ω_2 after some finite time at which point the foregoing analysis also applies. □

Theorem 1 states there are two equilibrium solutions, one unstable and the other AGES. The stable solution corresponds to a trailer being pulled while the unstable solution corresponds to a trailer being pushed. In both cases, the trailer equilibrium path is one with constant curvature, $\kappa_T^\star = \frac{\omega_T^\star}{\|\mathbf{v}_T^\star\|} = \frac{\kappa_L}{\sqrt{1-(\kappa_L \mathrm{d_x})^2}}$, i.e., similarly to the leader, the trailer describes a rectilinear or a circular path. The ratio $\frac{\kappa_T^\star}{\kappa_L}$ can be seen in Fig. 2 where the leader, in dashed red, describes a circular path and the follower, in dashed black, also describes a circular path but with larger curvature. The position of the follower w.r.t. $\{L\}$ (in red) is marked with ● and it depends on $\kappa_L \mathrm{d_x}$. If κ_L is much larger than $\mathrm{d_x}$ ($\kappa_L \mathrm{d_x} > 1$) no solution exists, but as explained in Remark 5 this should not be perceived as a disadvantage.

Theorem 2. *Consider a leader describing a path with constant curvature satisfying $\kappa_L \mathrm{d_x} = 1$ and a trailer attached to such leader. There is a unique equilibrium point which is not asymptotically stable.*

Proof. The same Lyapunov function as in Theorem 1 can be used with time derivative specified in (16). Under the conditions of the Theorem, $\cos(\psi^\star) = 0$ which means $V = 0$ cannot be asymptotically stable ($\dot{V}$ is not negative definite around the equilibrium point). □

In summary, for a leader describing a circular or a rectilinear path and given the conditions mentioned in Theorem 1, the trailer will converge to a unique solution for all initial conditions excluding a single unstable equilibrium point. Naturally, a question arises whether a similar result can be obtained for arbitrary paths.

5.3.3. Leader describing an arbitrary path

Previously, for a leader describing a circular path, a solution corresponding to an equilibrium point was found and it was shown that this equilibrium point is AGES. In particular, it is an almost global attractor, i.e. all other solutions (with the exception of the unstable equilibrium point) converge to it.

For a leader describing an arbitrary path, and under some conditions, we can also prove the existence of a unique attracting solution. The analytic expression for this solution (which is not an equilibrium point) will not be provided (as it is unknown) but, later on, we will be able to determine what this solution *resembles*.

Theorem 3. *Consider a leader describing a path with a time-varying curvature satisfying $|\kappa_L(t)\mathrm{d_x}|_\infty \leq \kappa_L^{\max}\mathrm{d_x} < 1$ and a trailer attached to the leader, initialized such that $\cos(\psi(0)) \geq -\sqrt{1-\kappa_L^{\max}\mathrm{d_x}}$. Then, $\cos(\psi(t))$ has a unique attracting solution.*

Proof. Under the conditions of the Theorem, Lemma 1 may be used (with $\epsilon = \sqrt{1-\kappa_L^{\max}\mathrm{d_x}}$) to conclude that after a finite time $\cos(\psi(t))$ will enter and not leave the interval $[\sqrt{1-\kappa_L^{\max}\mathrm{d_x}}\ 1]$. Consider now $\psi_1(t)$ and $\psi_2(t)$ as two solutions to (13) with different initial conditions. Without loss of generality, consider $\psi_1(0), \psi_2(0) \in]-\frac{\pi}{2}\ \frac{\pi}{2}[$ which is a positively invariant set as a consequence of Corollary 1. Now define the error angle, $\psi_e(t) = \psi_2(t) - \psi_1(t)$ (with $\psi_e(0) \neq 0$) whose dynamics, with the help of the Mean Value Theorem, can be written as $\dot{\psi}_e = -\frac{\mathrm{v}_L}{\mathrm{d_x}}(\sin(\psi_2) - \sin(\psi_1)) = -\frac{\mathrm{v}_L}{\mathrm{d_x}}\cos(\alpha)\psi_e$, where $\alpha \in [\min(\psi_2, \psi_1), \max(\psi_2, \psi_1)] \subset]-\frac{\pi}{2}\ \frac{\pi}{2}[$. Thus, $\psi_e = 0$ is an exponentially stable equilibrium point. □

Remark 6. The proof for Theorem 3 is closely related to contraction theory (Lohmiller & Slotine, 1998). In fact, for the dynamics (13) one finds that $\frac{\partial\dot{\psi}}{\partial\psi} = -\frac{\mathrm{v}_L}{\mathrm{d_x}}\cos(\psi)$, meaning that $\Omega = \{\psi : \cos(\psi) > \epsilon\}$ is a contraction region (remember that, under the conditions of the Theorem, $\Omega = \{\psi : \cos(\psi) > \epsilon\}$ is a positively invariant set and defines an ultimate bound for ψ).

From Theorem 3 one may conclude that the initialization of the trailer reference frame (under the above mentioned conditions) does not influence the final trailer reference frame, which means n followers can independently plan their trajectories as they will asymptotically behave as n points of a common trailer body. However, this is only valid for an upper bounded leader path

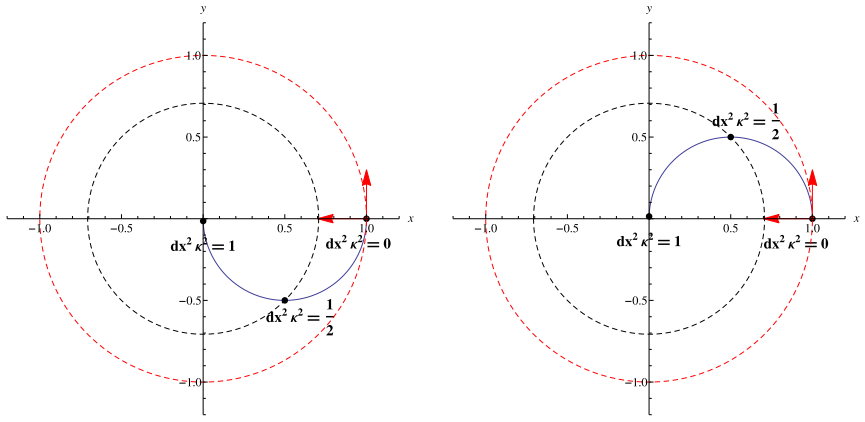

(a) AGES solutions (trailer being pulled). (b) Unstable solutions (trailer being pushed).

Fig. 2. Trailer equilibrium solutions for a leader describing a circular path (in red) for different combinations of $\kappa_L \mathrm{d_x}$.

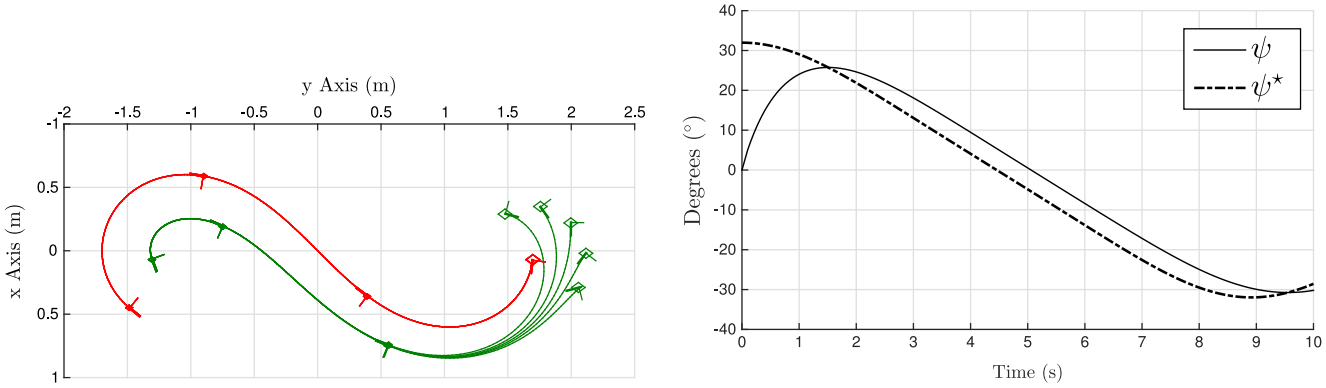

(a) *Virtual* follower's trajectories (in green) for different initializations. (b) Angle $\psi^\star$ and angle ψ for one of the initializations ($\psi(0) = 0°$).

Fig. 3. Leader describing lemniscate path (in red).

curvature (for reasons already discussed) and the trailer must be properly initialized (from Corollary 1, it is enough to initialize the trailer in a pulling position, which provides a wide range of initializations).

In Fig. 3, a simulation for a leader describing a lemniscate path is presented. In Fig. 3(a), the trajectories for different trailer initializations ($\psi(0) = \{\pm 80°, \pm 40°, 0°\}$) with $\mathrm{d_x} = 0.3$ m and $\mathbf{q} = [0\,0.3]^T$ m are shown, with the leader and trailer reference frames shown in red and green, respectively. Notice that all trajectories converge to one another in accordance with Theorem 3.

As mentioned before, Theorem 3 shows that a unique attracting trajectory exists but it does not provide any insight on what that solution looks like. Fig. 3(b) shows the angle ψ obtained from solving (13) with $\psi(0) = 0$, and the angle $\psi^\star$ given by (15a) with time varying $\kappa_L(t)$ corresponding to the lemniscate path. Notice that ψ *tries to follow* $\psi^\star$ but with a certain time delay, as if ψ were trying to converge to $\psi^\star$. The next section provides useful insight into the *closeness* between ψ to $\psi^\star$.

5.3.4. Characterizing the trailer solution for arbitrary leader paths

For a leader describing a path where the curvature varies slowly with the arc-length, one expects the trailer to behave as if the leader were describing a quasi-circular path, i.e. if a *large enough* portion of the leader path resembles a portion of a circular path, the trailer attracting reference frame (see Theorem 3) should be close to the equilibrium solution that would be obtained if the leader were actually describing a circular path. In this section, we provide conditions that characterize the distance between ψ and the solution $\psi^\star$ given by (15a). Notice that, here we are using $\psi^\star$ with a different interpretation from that of Section 5.3.2, though the expression remains the same. While for the case of constant curvature paths, $\psi^\star$ defines the attracting solution, when the curvature is time-varying, $\psi^\star$ and the attracting solution no longer coincide. Intuition suggests that when $\kappa_L^{\max}\mathrm{d_x}$ is close to one, the rate of change of κ_L (w.r.t. the path's arc length) must be small to allow for ψ to get close to $\psi^\star$. As $\kappa_L^{\max}\mathrm{d_x}$ decreases, larger variations in curvature can be accommodated, without compromising the ability to *track* $\psi^\star$. The rate of change of the leader path curvature with the leader path parametrization, κ_L', is defined as $\kappa_L' \equiv \frac{d\kappa_L}{dt}\frac{1}{\mathrm{v_L}}$.

The following theorem provides conditions under which an explicit bound on the distance between ψ and $\psi^\star$ is guaranteed to ultimately hold.

Theorem 4. *Consider a leader describing a path with a time-varying curvature satisfying* $-1 < \kappa_L^{\min}\mathrm{d_x} \leq \kappa_L(t)\mathrm{d_x} \leq \kappa_L^{\max}\mathrm{d_x} < 1$, *and* $|\kappa_L'| \leq \kappa_L'^{\infty}$. *Additionally, consider a trailer attached to the leader initialized such that* $\cos(\psi(0)) \geq 0$, *with motion described by* (13). *Under those conditions,*

$$\cos(\psi - \psi^\star) \geq \frac{1 - C^2}{1 + C^2} \tag{18}$$

defines an invariant set and an ultimate bound on ψ, *where* $C = \frac{1}{2}\frac{\kappa_L'^{\infty}\mathrm{d_x^2}}{1-\kappa_L^{\max}\mathrm{d_x}}$ *and* $\psi^\star$ *satisfies* (15a). *Additionally,*

$$-\kappa_L^{\max}\mathrm{d_x} \leq \sin\big(\psi(t)\big) \leq -\kappa_L^{\min}\mathrm{d_x}, \tag{19}$$

also defines an invariant set and an ultimate bound.

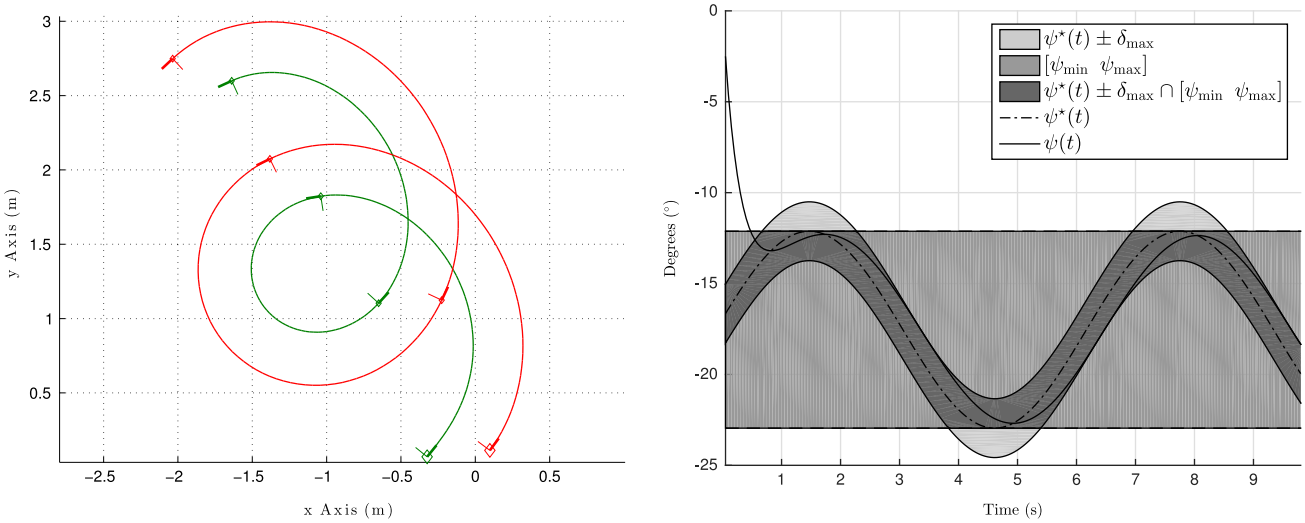

(a) *Virtual* follower and leader trajectories, in green and red, respectively.

(b) Angles ψ, $\psi^\star$ and bounds determined from (18) and (19).

Fig. 4. Leader describing a path (in red) with curvature that varies sinusoidally with the arc-length.

Proof. Consider the stable equilibrium solution $\psi^\star$ in (15a), with dynamics given by

$$\dot{\psi}^\star = -\frac{\mathrm{v}_L}{\mathrm{d_x}} \frac{\kappa_L' \mathrm{d_x}^2}{\sqrt{1-(\kappa_L \mathrm{d_x})^2}}. \tag{20}$$

Consider the positive definite Lyapunov function $V = 1-\cos(\psi-\psi^\star)$, whose time derivative, with the help of (13) and (20), can be seen to satisfy

$$\dot{V} \leq -\frac{\mathrm{v}_L}{\mathrm{d_x}}(\cos(\psi)+\cos(\psi^\star))\left(V - |\sin(\psi-\psi^\star)|C\right). \tag{21}$$

Under the conditions of the Theorem, $\cos(\psi)$ is positive (from Lemma 1) and by definition $\cos(\psi^\star)$ is also positive (see (15a)). Consequently, the derivative (21) is negative definite while $V - |\sin(\psi-\psi^\star)|C > 0 \Leftrightarrow \cos(\psi-\psi^\star) < \frac{1-C^2}{1+C^2}$, which means $\cos(\psi-\psi^\star)$ must necessarily evolve until $\cos(\psi-\psi^\star) \geq \frac{1-C^2}{1+C^2}$ (or equivalently, V must evolve until $V \leq \frac{2C^2}{1+C^2}$), from which point in time such condition is forever satisfied. Due to paper length limitations, details on the derivation of (21) are omitted.

Now, consider the time derivative of $\sin(\psi)$, which renders $\frac{d}{dt}\sin(\psi) = -\frac{\mathrm{v}_L}{\mathrm{d_x}}\cos(\psi)(\sin(\psi)+\kappa_L \mathrm{d_x})$, where $\cos(\psi)$ is definite positive as explained before. The time derivative is negative while $\sin(\psi) > -\kappa_L^{\min}\mathrm{d_x}$ and positive when $\sin(\psi) < -\kappa_L^{\max}\mathrm{d_x}$, proving convergence to the interval (19). □

Remark 7. Theorem 4 extends Theorem 1 to consider time-varying curvatures, in the sense that the latter is partially recovered if the condition $\kappa_L' = 0$ is imposed. For that case, $\cos(\psi-\psi^\star) \geq 1$ and $-\kappa_L \mathrm{d_x} \leq \sin\big(\psi(t)\big) \leq -\kappa_L \mathrm{d_x}$ (as $\kappa_L^{\max} = \kappa_L^{\min} = \kappa_L$). Notice however that the estimate for the region of attraction provided by Theorem 4 is smaller than the almost global domain specified in Theorem 1.

As a consequence of (18), the smaller the constant C the closer ψ is to $\psi^\star$ as a consequence of (18). The constant C is smaller for smaller values of $|\kappa_L'|$ and for smaller values of $\kappa_L^{\max}\mathrm{d_x}$. With that in mind, Theorem 4 says that whatever the attracting solution is, the closer a leader is to describing a circular path, the closer the trailer trajectory will be to the solution (15a) (it does not matter how fast the curvature changes in time, but rather how fast it changes with the arc-length). The distance between the two solutions also depends on $\kappa_L^{\max}\mathrm{d_x}$, for reasons already discussed.

In Fig. 4, a leader describes a path where the curvature varies sinusoidally with the arc-length and is such that $\{\kappa_L^{\min}, \kappa_L^{\max}\} = \{-1.3, -0.7\}\ \mathrm{m}^{-1}$ and $\kappa_L'^{\infty} = 0.3\ \mathrm{m}^{-2}$ with $\mathrm{d_x} = 0.3$ m and $\mathbf{q} = [0\ 0.3]^T$ m. Fig. 4 shows the leader's and *virtual* follower's trajectories (the impact of the initialization $\psi(0) = 0$ vanishes in time/arc-length). Fig. 4(b) presents the angles ψ and $\psi^\star$ and the bounds that follow from (18) and (19) (these bounds are ultimate bounds with ψ reaching them in finite time). Each bound may be more restrictive than the other and combining both we find a less conservative bound, represented by the darker region in Fig. 4(b). As such, that darker region provides us with some knowledge of what the attracting solution resembles.

Theorem 5. *Consider a leader describing a path with a time-varying curvature satisfying* $|\kappa_L(t)\mathrm{d_x}| \leq \kappa_L^{\max}\mathrm{d_x} < 1$. *Additionally, consider a trailer attached to the leader with motion described by* (13) *but where the leader velocity measurements are corrupted, i.e.* $\hat{\mathbf{v}}_L = \mathbf{v}_L + \mathrm{v}_L\boldsymbol{\delta}_v$. *Assume the path curvature associated with the corrupted velocity* $\hat{\kappa}_L$ *satisfies* $\left|\hat{\kappa}_L(t)\mathrm{d_x}\right| \leq \kappa_L^{\max}\mathrm{d_x} < 1$ *and that the trailer starts in a pulling position. Under those conditions* $\cos(\hat{\psi}-\psi) \geq \frac{1-C^2}{1+C^2}$ *defines an ultimate bound and invariant set, where* $\cos(\hat{\psi})$ *encodes the trailer with corrupted measurements,* $\cos(\psi)$ *encodes the attracting trailer defined in Theorem 3 and* $C = \frac{1}{2}\frac{\|\boldsymbol{\delta}_v\|}{\sqrt{1-\kappa_L^{\max}\mathrm{d_x}}}$. *Moreover, if* $\exists T \geq 0 : \forall t \geq T\, \boldsymbol{\delta}_v(t) = 0$, *then* $\lim_{t\to\infty}\cos(\hat{\psi}-\psi) = 0$.

Proof. The proof follows very closely that of Theorem 4. Given the conditions of the Theorem, Lemma 1 guarantees $\cos(\hat{\psi}) \geq \sqrt{1-\kappa_L^{\max}\mathrm{d_x}}$ and $\cos(\psi) \geq \sqrt{1-\kappa_L^{\max}\mathrm{d_x}}$. Also the kinematics of the corrupted trailer render (see (10))

$$\hat{\omega}_T(t) = \frac{\mathbf{e_2}^T\,{}_I^T R(\hat{\psi})\hat{\mathbf{v}}_L}{\mathrm{d_x}} = \frac{\mathbf{e_2}^T\,{}_I^T R(\hat{\psi})\mathbf{v}_L}{\mathrm{d_x}} + \frac{\mathbf{e_2}^T\,{}_I^T R(\hat{\psi})\mathrm{v}_L\boldsymbol{\delta}_v}{\mathrm{d_x}},$$

where ${}_T^I R(\hat{\psi})$ is the corrupted trailer rotation matrix. It then follows $\dot{\hat{\psi}} = \hat{\omega}_T - \omega_L = -\frac{\mathrm{v}_L}{\mathrm{d_x}}(\sin(\hat{\psi}) + \kappa_L\mathrm{d_x} + \mathbf{e_2}^T\,{}_I^T R(\hat{\psi})\boldsymbol{\delta}_v)$, and following the same steps as in Theorem 4, the ultimate bound and invariant set is found based on the maximum of $\|\boldsymbol{\delta}_v\|$, which is defined such that $\hat{\kappa}_L \leq \kappa_L^{\max}$. The final conclusion of the Theorem is a direct consequence of Theorem 3. □

Theorem 5 guarantees that n followers can perform their planning independently, since bounded noise on the velocity measurements produces bounded errors on the trailer's attitude relative

to the nominal solution. Moreover, the presence of noise does not have a long lasting effect, in the sense that as soon as the noise vanishes to zero, the attitude error also decays to zero.

Remark 8. Notice that if we impose a motion to a trailer, we can find the leader motion with the help of (8) (indeed, if $d_y = 0$, then $\mathbf{p}_L = \mathbf{p}_T + \frac{\mathbf{v}_T}{\|\mathbf{v}_T\|} d_x$). In fact, the system trailer and leader is differentially flat with the trailer position as the flat output (Fliess, Lévine, Martin, & Rouchon, 1995; Levine, 2009). Recall that, in the framework of our paper, the trailer encapsulates the motion of a formation of n vehicles, as n distinct points of the trailer, while the leader guides the motion of the trailer. Also, from Theorem 3, it follows that, given a $\kappa_L(t)$, a unique attracting $\kappa_T(t)$ exists; conversely, given $\kappa_T(t)$ (and $\dot{\kappa}_T(t)$), a unique $\kappa_L(t)$ also exists (see Fliess et al., 1995, Section 4.2). Thus, in applications where a formation is required to move as a fixed geometrical formation, encoded by $\mathbf{p}_T^\star$, it suffices to force the leader to describe the motion resulting from (8) given $\mathbf{p}_T^\star$, and we show that the trailer motion $\mathbf{p}_T$ is attracted to $\mathbf{p}_T^\star$, provided that the trailer is initialized in a domain of attraction (see Theorem 3 and Fig. 3(a)), which is more powerful than simply having a nominal solution.

Remark 9. The proposed planner does not mimic the leader's motion, thus, in general, higher velocities and accelerations than the leader's are required from the *real* follower. There exist bounds on the planned velocity and acceleration as functions of the leader's velocity and acceleration, and, thus, given bounds on the follower's performance, bounds on the leader trajectory can be imposed that guarantee that the follower planned trajectory is feasible.

6. Experiments

6.1. Experimental setup

For the experimental validation of the proposed algorithm, the architecture uses a MATLAB/Simulink environment to seamlessly integrate the sensors, the control algorithm, and the communication with the vehicle. The proposed trajectory planner was tested with two radio controlled Blade mQX quadrotor vehicles (BlademQX, 2013). A VICON T-Series motion capture system (VICON, 2013), composed of 12 T-Series cameras and markers attached to the quadrotors, provides highly accurate position and orientation measurements for the leader and follower at a rate of 100 Hz. The trajectory planner is implemented in a Matlab/Simulink model, which computes the follower's position reference and feeds it to the quadrotors's trajectory tracker controller developed in Cabecinhas, Cunha, and Silvestre (2012) which requires a time-parametrized position reference of class C^3. Consequently, the trajectory planner requires the knowledge of $\mathbf{p}_L^{(i)}(t)$ for $i = \{1, 2, 3\}$, which are obtained from the raw position measurements by means of dynamic differentiators.

6.2. Experiments

Two experiments are presented, where the leader's path is depicted in red, the *real* follower's path in blue and the *virtual* follower's path in magenta, with the magenta reference frame being that of the virtual follower, i.e. ${}^I_F R$. In Figs. 5(a)–(c) and 6(a), the vehicles' positions are shown five times, using the symbol $\diamond$ for the initial position and the symbol $\bullet$ for the other positions, equally spaced in time (elapsed time divided by four). In all experiments, the leader's velocity was set at 0.5 ms^{-1}.

The angles ψ and $\psi^\star$ are presented in dashed and full lines, respectively in Figs. 5(d) and 6(d), with $\psi^\star$ computed from (15a) and ψ computed from ${}^L_T R = {}^L_I R \, {}^I_T R$, where ${}^L_I R$ is the leader frenet reference frame for the motion along the plane orthogonal to $\mathbf{n}$.

Fig. 5(a)–(c) depict the paths for $d_x = 0.4$ m, $\mathbf{d} = [0\ 0.4]^T$ m, $d_z = 0$ m and $\mathbf{n} = \mathbf{e}_3$. The leader quadrotor describes a path composed of two circular paths: one in a horizontal plane and the other in a plane tilted 45°. As a consequence, for the circular path in the horizontal plane, the leader pulling the trailer is describing a circle (thus Theorem 1 applies). However, for the circular path in the tilted plane, the leader pulling the trailer is describing an ellipse. For the first case, the *virtual* follower converges to a circular path as expected and $\psi^\star$ is a constant ($\approx -23.6°$) to which ψ converges to, as can be seen in Fig. 5(d). For the second case, $\psi^\star$ is not a constant (in an ellipse, the path curvature changes) and ψ *tries to follow it*, which can also be verified in Fig. 5(d). The planning along $\mathbf{n}$ is trivial, with the *virtual* follower keeping the same altitude as the leader's, clearly perceptible in Fig. 5(a)–(c). In Fig. 6(a), $d_x = 0.35$ m, $\mathbf{d} = [0\,0.35]^T$ m, $d_z = 0.35$ m and $\mathbf{n} = R_y(15°)R_z(-45°)\mathbf{e}_3 \equiv R\mathbf{e}_3$. The leader quadrotor describes a lemniscate path in a plane tilted 15°, defined as $\mathbf{p}(\gamma) = 1.7\,R[\frac{\cos(\gamma)}{1+\sin^2(\gamma)} \ \frac{1}{2}\frac{\sin(2\gamma)}{1+\sin^2(\gamma)} \ -1.1]^T$ (m). The leader's path is not circular and as a consequence ψ and $\psi^\star$ vary in time, as can be seen in Fig. 6(c). Notice that the planned trajectory is a rich one, in the sense that it is not a mere copy of the leader's. Moreover, when the leader describes a clockwise motion (w.r.t. $\mathbf{n}$) the *virtual* follower path has a larger curvature (than the trailer's hinge point) and when the leader describes an anti-clockwise motion the *virtual* follower path has a smaller curvature, which is a consequence of modeling the *virtual* follower as a point of a rigid body. In Fig. 6d the tracking position error is presented, once again with convergence of the blue line to the magenta line. Notice that the planner has been provided with an appropriate $\mathbf{n}$ (in fact, it was provided with the normal to the leader plane of motion). Had $\mathbf{n}$ been selected differently, the planning would have been different and perhaps more unintuitive.

7. Conclusions

In this paper, a real-time three dimensional trajectory planner for leader following was presented. The proposed trajectory planner is intuitive and can be implemented independently by each follower, thus reducing the need for communications among vehicles. Each follower vehicle behaves as a point of a two dimensional rigid body trailer rigidly attached to a leader vehicle. We proved that under a wide range of conditions, there is a unique attractive solution for the trailer reference frame to which all solutions converge, which demonstrates the robustness of the planning to disturbances and different initializations. Moreover, bounds on the planned velocity and acceleration can be used in limiting the leader's velocity and acceleration with the intent of guaranteeing that the planned trajectories are feasible for all followers. Experiments performed with quadrotor vehicles were conducted that demonstrate the richness and suitability of the generated trajectories. Directions for future work include the study of a sequence of n-trailers and the incorporation of a collision avoidance strategy.

Acknowledgments

This work was partially supported by the project MYRG2015-00126-FST of the University of Macau, by the Macao Science and Technology Development Fund under Grant FDCT/048/2014/A1, and by the Portuguese Fundacão para a Ciência e a Tecnologia (FCT) through Institute for Systems and Robotics (ISR), under Laboratory for Robotics and Engineering Systems (LARSyS) (UID/EEA/50009/2013) and through Institute for Mechanical Engineering (IDMEC), under Associated Laboratory for Energy, Transports and Aeronautics (LAETA) (UID/EMS/50022/2013) projects.

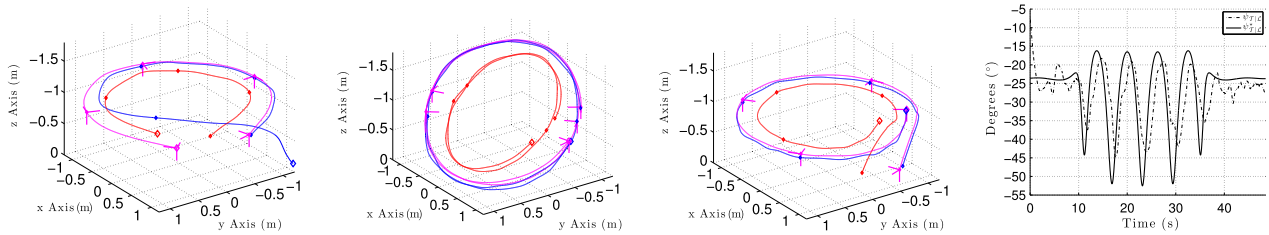

(a) Trajectories from 0 to 11 s. (b) Trajectories from 11 to 35 s. (c) Trajectories from 35 to 48.5 s. (d) Angles ψ and $\psi^{\star}$.

Fig. 5. Leader describing (in red) circular path in planes tilted 0° and 45°.

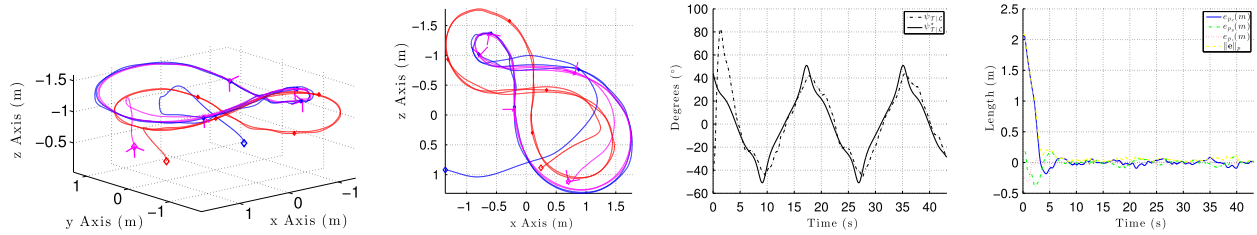

(a) Trajectories. (b) Trajectories top view. (c) Angles ψ and $\psi^{\star}$. (d) Tracking position error between *virtual* and *real* follower.

Fig. 6. Leader describing (in red) lemniscate path in plane tilted 15°.

The work of R. Cunha was supported by the FCT Investigator Programme under Contract IF/00921/2013 and PTDC/EEI-AUT/5048/2014. Carlos Silvestre is on leave from the Instituto Superior Técnico, Universidade de Lisboa, Lisboa, Portugal.

References

Balch, T., & Arkin, R. C. (1999). Behavior-based formation control for multi-robot teams. *Transactions on Robotics and Automation*, *14*, 926–939.

Bellingham, J. G., & Rajan, K. (2007). Robotics in remote and hostile environments. *Science*, *318*(5853), 1098–1102.

BlademQX (2013). Quadrotor specifications: www.bladehelis.com. September.

Cabecinhas, D., Cunha, R., & Silvestre, C. (2012). Saturated output feedback control of a quadrotor aircraft. In *American control conf.*, (pp. 4667–4602).

Consolini, L., Morbidi, F., Prattichizzo, D., & Tosques, M. (2008). Leader–follower formation control of nonholonomic mobile robots with input constraints. *Automatica*, *44*(5), 1343–1349.

Cui, R., Sam Ge, S., How, B., & Choo, Y. (2010). Leader follower formation control of underactuated autonomous underwater vehicles. *Ocean Engineering*, *37*, 1491–1502.

Do, K. D., & Pan, J. (2007). Nonlinear formation control of unicycle-type mobile robots. *Robotics and Autonomous Systems*, *55*(3), 191–204.

Fink, J., Michael, N., Kim, S., & Kumar, V. (2011). Planning and control for cooperative manipulation and transportation with aerial robots. *The International Journal of Robotics Research*, *30*(3).

Fliess, M., Lévine, J., Martin, P., & Rouchon, P. (1995). Flatness and defect of non-linear systems: introductory theory and examples. *International Journal of Control*, *61*(6), 1327–1361.

Hua, M., Hamel, T., Morin, P., & Samson, C. (2013). Introduction to feedback control of underactuated VTOL vehicles: A review of basic control design ideas and principles. *Control Systems*, *33*(1), 61–75.

Justh, E. W., & Krishnaprasad, P. S. (2004). Equilibria and steering laws for planar formations. *Systems & Control Letters*, *52*(1), 25–38.

Lawton, J. R. T., Beard, R. W., & Young, B. J. (2003). A decentralized approach to formation maneuvers. *Transactions on Robotics and Automation*, *19*(6), 933–941.

Leonard, Naomi Ehrich, & Fiorelli, Edward (2001). Virtual leaders, artificial potentials and coordinated control of groups. In *Conf. on decision and control, vol. 3* (pp. 2968–2973). IEEE.

Levine, J. (2009). *Analysis and control of nonlinear systems: A flatness-based approach*. Springer Science & Business Media.

Lohmiller, W., & Slotine, J. E. (1998). On contraction analysis for non-linear systems. *Automatica*, *34*(6), 683–696.

Mariottini, G.L., Morbidi, F., Prattichizzo, D., Pappas, G.J., & Daniilidis, K. (2007). Leader-follower formations: Uncalibrated vision-based localization and control. In *International conf. on robotics and automation*, (pp. 2403–2408).

Peng, Z., Wen, G., Rahmani, A., & Yu, Y. (2013). Leader–follower formation control of nonholonomic mobile robots based on a bioinspired neurodynamic based approach. *Robotics and Autonomous Systems*,.

Pereira, P., Cunha, R., Cabecinhas, D., Silvestre, C., & Oliveira, P. (2014). Trailer-like leader following trajectory planning. In *Conf. on decision and control*.

Roldão, V., Cunha, R., Cabecinhas, D., Oliveira, P., & Silvestre, C. (2013). A novel leader-following strategy applied to formations of quadrotors. In *European control conf.*.

Summers, T.H., Yu, C., & Anderson, B.D. (2008). Robustness to agent loss in vehicle formations and sensor networks. In *Conf. on decision and control*, (pp. 1193–1199).

VICON. (2013). Vicon system: http://www.vicon.com. September.

Wen, G., Peng, Z., Yu, Y., & Rahmani, A. (2012). Planning and control of three-dimensional multi-agent formations. *IMA Journal of Mathematical Control and Information*,.

Yamaguchi, H. (2002) A distributed motion coordination strategy for multiple nonholonomic mobile robots in cooperative hunting operations. In *Conf. on decision and control, vol. 3*, (pp. 2984–2991).

Pedro O. Pereira received the M.Sc. degree in Aerospace Engineering from the Instituto Superior Técnico (IST) and the Delft University of Technology (TU Delft) in 2013. He is currently a Ph.D. candidate at the department of Automatic Control in the Royal Institute of Technology (KTH). His research interests include nonlinear control and motion planning for aerial vehicles.

Rita Cunha received the Licenciatura degree in Information Systems and Computer Engineering and the Ph.D. degree in Electrical and Computer Engineering from the Instituto Superior Técnico (IST), Universidade de Lisboa, Portugal, in 1998 and 2007, respectively. She is currently an Assistant Researcher with the Institute for Systems and Robotics, LARSyS, Lisbon, and an Invited Assistant Professor with the Department of Electrical and Computer Engineering of IST. Her research interests include nonlinear systems and control, vision-based and laser-based control with application to autonomous air vehicles.

David Cabecinhas received the Licenciatura and Ph.D. degrees in electrical and computer engineering from the Instituto Superior Técnico, Lisbon, Portugal, in 2006 and 2014, respectively. He has been a researcher with the Laboratory of Robotics and Systems in Engineering and Science, Institute for Systems and Robotics, Lisbon, since 2007. He is currently a Post-Doctoral Fellow with the Faculty of Science and Technology, University of Macau, Macau, China. His current research interests include nonlinear control, sensor-based and vision-based control with applications to autonomous aerial and surface vehicles, and modeling and identification of aerial and surface vehicles.

Carlos Silvestre received the Licenciatura degree in Electrical Engineering from the Instituto Superior Tecnico (IST) of Lisbon, Portugal, in 1987 and the M.Sc. degree in Electrical Engineering and the Ph.D. degree in Control Science from the same school in 1991 and 2000, respectively. In 2011, he received the Habilitation in Electrical Engineering and Computers also from IST. Since 2000, he is with the Department of Electrical Engineering of the Instituto Superior Tecnico, where he is currently an Associate Professor of Control and Robotics on leave. Since 2015, he is a professor of the Department of Electrical and Computers Engineering of the Faculty of Science and Technology of the University of Macau. Over the past years, he has conducted research on the subjects of navigation guidance and control of air and underwater robots. His research interests include linear and nonlinear control theory, coordinated control of multiple vehicles, gain scheduled control, integrated design of guidance and control systems, inertial navigation systems, and mission control and real time architectures for complex autonomous systems with applications to unmanned air and underwater vehicles.

Paulo Oliveira received the Ph.D. degree in Electrical and Computer Engineering, from the Instituto Superior Técnico (IST), Lisbon, Portugal, in 2002. He is an Associate Professor in the Department of Mechanical Engineering of IST and researcher in the Institute of Mechanical Engineering, IST. He also collaborates with the Institute for Systems and Robotics, IST. His areas of scientific activity are Mechatronics with special focus on the fields of Autonomous Vehicles, Robotics, Sensor Fusion, Navigation, Positioning, and Nonlinear Estimation. Over the last 25 years, he participated in more than 30 European and Portuguese research projects and he co-authored more than 200 journal and conference papers.